Journal of Solid Mechanics Vol. 8, No. 4 (2016) pp. 875-894

Lateral Vibrations of Single-Layered Graphene Sheets Using Doublet Mechanics

A. Fatahi-Vajari , A. Imam *

Department of Mechanical and Aerospace Engineering, Science and Research Branch, Islamic Azad University, Tehran, Iran

Received 1 August 2016; accepted 8 October 2016

ABSTRACT

This paper investigates the lateral vibration of single-layered graphene sheets based on a new theory called doublet mechanics with a length scale parameter. After a brief reviewing of doublet mechanics fundamentals, a sixth order partial differential equation that governs the lateral vibration of single-layered graphene sheets is derived. Using doublet mechanics, the relation between natural frequency and length scale parameter is obtained in the lateral mode of vibration for single-layered graphene. It is shown that length scale parameter plays a significant role in the lateral vibration behavior of single-layered graphene sheets. Such effect decreases the natural frequency compared to the predictions of the classical continuum mechanics models. However with increasing the length of the plate, the effect of scale parameter on the natural frequency decreases. For validating the results of this method, the results obtained herein are compared with the existing nonlocal and molecular dynamics results and good agreement with the latter is observed.

Keywords : Doublet mechanics; Natural frequency; Length scale parameter; Lateral vibration; Single-layered graphene sheets.

1 INTRODUCTION

AT nanoscale, the mechanical characteristics of nanostructures are often significantly different from their behavior at macroscopic scale due to the inherent size effects. Such effects are essential for nanoscale materials or structures and the influence on nanoinstruments is great. Size effects exist not only for mechanical properties but also for electronic, optical and some other properties.

One particular theory that has recently been applied to materials with microstructure is doublet mechanics (DM). This approach originally developed by Granik [1], has been applied to granular materials by Granik, Ferrari [2] and Ferrari et al. [3]. DM is a micromechanical discrete model whereby solids are represented as arrays of points, particles or nodes at finite distances. The theory has shown promise in predicting observed behaviors that are not predictable using continuum mechanics. These behaviors include the so-called Flamant paradox (Ferrari et al.) [3], where in a half-space under compressive boundary loading, continuum theory predicts a completely compressive stress field while observations indicate regions of tensile stress. Other anomalous behaviors include dispersive wave propagation. Ferrari et al. reformulated DM using a finite element approach with the aim of further expanding the potential applications of this theory [4]. Some application of doublet mechanics in biomedical nanomechanics is given in [5-7] and for civil engineering is given in [8, 9]. Fang et al. [10] studied the plane wave propagation in a cubic tetrahedral assembly with DM. Some other application of doublet mechanics is given in [11].

*Corresponding author. Tel.: +982144869442; Fax.: +982144869442.
E-mail address: aimam@srbiau.ac.ir (A. Imam).

One of the most popular approaches to micromechanics is via nonlocal theory. The nonlocal elasticity theory as developed by Eringen [12] assumes that the stress tensor at a point is a function of strains at all points in the continuum. It is different from the classical continuum theory because the latter is based on constitutive relation which states that the stress at a point is a function of strain at that particular point. Another popular theory used in micromechanics is molecular dynamics (MD) theory. This theory studies vibrations of the atomic nuclei of solid crystals, the nuclei being considered as material points (particles) mutually bonded by elastic interatomic forces [3]. Carbon nanotubes (CNTs) have been invented by Iijima in 1991 [13]. The production of nanostructure is explained in [14-16]. CNTs have many important characteristics, notable among which are mechanical behavior in the design of micro electro-mechanical systems (MEMS) and nano electromechanical systems (NEMS) [17]. Danesh et al. [17] studied the small scale effect on the axial vibration of a tapered nanorod employing nonlocal elasticity theory, where differential quadrature method (DQM) is applied to solve the governing equations of the nanorod for different boundary conditions. Wang and Wang [18] presented the constitutive relations of nonlocal elasticity theory for application in the analysis of CNTs when modelled as Euler–Bernoulli beams, Timoshenko beams or as cylindrical shells. Ghannadpour et al. [19] investigated the bending, buckling and vibration analyzes of nonlocal Euler beams using Ritz method to analyze the nonlocal beams with arbitrary boundary conditions. Malekzadeh et al. [20] investigated the small size effect on the free vibration behavior of finite length nanotubes embedded in an elastic medium based on the three-dimensional (3D) nonlocal elasticity theory.

The investigation of single-layered graphene sheets (SLGSs) is of great importance on the nanoscale, since CNTs are assumed to be as deformed graphene sheets. Graphene is the first example of a truly two-dimensional crystal that has only one layer of carbon atoms [21, 22]. The vibrational characteristics of SLGSs are attracting increasing attention since they may be used as nanosensor and nanoactuator. Continuum elastic mechanical models [23, 24] used to study vibration of SLGSs do not consider scale effects while the nonlocal continuum modeling and molecular structural mechanics approach as applied to vibration of carbon nanoplates [25- 35] do consider scale effects. Reddy [25] reformulated the classical and shear deformation beam and plate theories using the nonlocal differential constitutive relations of Eringen and the von Karman nonlinear strains. Aghababaei and Reddy [26] reformulated the third-order shear deformation plate theory of Reddy using the nonlocal linear elasticity theory of Eringen with ability to capture both the small scale effects and the quadratic variation of shear strain and consequently shear stress through the plate thickness. Farajpour et al. in [27] studied the buckling behavior of circular SLGS under uniform radial compression considering small-scale effect using nonlocal elasticity theory. Pradhan and Phadikar [28] reformulated classical plate theory (CLPT) and first-order shear deformation theory (FSDT) of plates using the nonlocal differential constitutive relations of Eringen using Navier's approach to solve the governing equations for simply supported boundary conditions. Alibeigloo [29] studied vibration analysis of a nano-plate, based on three-dimensional theory of elasticity, employing non-local continuum mechanics. Aksencer and Aydogdu [30] studied buckling and vibration of nanoplates using nonlocal elasticity theory by applying Navier type solution for simply supported plates and Levy type method for plates with two opposite edge being simply supported and the remaining ones arbitrary. Ansari et al. [31] investigated vibration analysis of rectangular SLGSs via nonlocal continuum plate model using classical Mindlin plate theory. Jalali et al. [32] based on nonlocal differential constitutive relations of Eringen, reformulated the first order shear deformation theory of plates (FSDT) for vibration of nanoplates considering the initial geometric imperfection. Rouhi and Ansari [33] developed a nonlocal plate model which accounts for the small scale effects to study the vibrational characteristics of multi-layered graphene sheets with different boundary conditions embedded in an elastic medium. Aksencer and Aydogdu [34] investigated forced vibration of nanoplates using the nonlocal elasticity theory using Navier type solution method for simply supported nanoplates.

Vibration analysis of nano-rectangular plates based on DM has not yet been investigated analytically, and the present work attempts to consider this analysis. The purpose of this study is to study lateral vibration of SLGSs using DM. The basic equation of motion for lateral vibration of SLGSs which considers small scale effect is obtained. After briefly reviewing the basics of DM, this theory is applied to obtain frequency equation for lateral vibration of SLGSs.

2 BRIEF REVIEW OF DM

2.1 Fundamental equations

Originally developed by Granik [1], DM is a micromechanical theory based on a discrete material model whereby solids are represented as arrays of points or nodes at finite distances. A pair of such nodes is referred to as a doublet, and the nodal spacing distances introduce length scales into the microstructural theory. Each node in the array is allowed to have translation and rotation where small translational and rotational displacements are expanded in Taylor series about the nodal point. The order at which the series is truncated defines the degree of approximation employed. The lowest order case using only a single term in the series does not contain any length scales, while using the terms beyond the first will produce a multi length scale theory. In this way, kinematical microstrains of elongation, shear and torsion (about the doublet axis) are developed. Through appropriate constitutive assumptions, such microstrains can be related to corresponding elongational, shear and torsional microstresses.

A doublet being a basic constitutive unit in DM is shown in Fig. 1. Corresponding to the doublet *(A, B)* there exists a doublet or branch vector ζ_a connecting the adjacent particle centers and defining the doublet axis. The magnitude of this vector $\eta_a = |\zeta_a|$ is simply the particle diameter for particles in contact. However in general, the particles need not be in contact and for this case the length scale η_a could be used to represent a more general microstructural feature.

As mentioned above, the kinematics allow relative elongational, shearing and torsional motions between the particles, and this is used to develop an elongational microstress p_a, shear microstress t_a, and torsional microstress m_a as shown in Fig. 1. It should be pointed out that these microstresses are not second order tensors in the usual continuum mechanics sense. Rather, they are vector quantities that represent the elastic microforces and microcouples of interaction between doublet particles an example of which is interatomic forces between carbon molecules of a nanoplate. Their directions are dependent on the doublet axes which are determined by the material microstructure.

In Fig. 2, suppose doublet (a, b_α) transforms to doublet $(a', b_\alpha^{'})$ as a result of kinematic translation. The superscript 0 for vectors indicates the initial configuration.

If $u(x,t)$ is the displacement field coinciding with a particle displacement, then the incremental displacement is written as:

$$\Delta u_\alpha = u\left(x + \zeta_\alpha^0, t\right) - u\left(x, t\right) \tag{1}$$

where *x* is the position vector of particle.

Here, $\alpha = 1, ..., n$ while *n* is referred to the numbers of doublets. For the problem under study, it is assumed that the shear and torsional microdeformations and microstresses are negligible and thus only extensional strains and stresses exist.

As in linear elasticity, it is assumed that the relative displacement Δu_α is small compared to the doublet separation distance η_α ($|\Delta u_\alpha| \prec\prec \eta_\alpha$) as a result of which it may be concluded that $\tau_\alpha = \tau_\alpha^0$ [3].

The extensional microstrain scalar measure ε_α, representing the axial deformation of the doublet vector, is defined as [3]:

$$\varepsilon_\alpha = \frac{\tau_\alpha . \Delta u_\alpha}{\eta_\alpha} \tag{2}$$

The incremental function in Eq. (2) can be expanded in a Taylor series as [3]:

$$\varepsilon_\alpha = \tau_\alpha^0 . \sum_{x=1}^{M} \frac{\left(\eta_\alpha\right)^{\chi-1}}{x!} (\tau_\alpha^0 . \nabla)^x u \tag{3}$$

where ∇ is the Del operator in general coordinates. The η is the internal characteristic length scale. As mentioned above, the number of terms used in the series expansion determines the order of the approximation in DM theory. In DM under such assumptions and neglecting temperature effect, the relation between microstrain and microstress is written as below [3].

$$p_\alpha = \sum_{\beta=1}^{n} A_{\alpha\beta} \varepsilon_\beta \tag{4}$$

where p_α is the axial microstress along doublet axes. An example of the axial microstress is the interatomic forces between atoms or molecules located at the nodes of a general array such as a crystalline lattice. In the case of linear and homogeneous inter-nodal central interactions, Eq. (4) can be interpreted as the constitutive equation in the linear and homogeneous DM theory, and $A_{\alpha\beta}$ is the matrix of the micromodules of the doublet.

It may be written $\tau_\alpha^0 = \tau_{\alpha j}^0 e_j$ where $\tau_{\alpha j}^0$ are the cosines of the angles between the directions of microstress and the coordinates and $\{e_i\}$ are the unit vectors in Cartesian coordinate.

In the homogeneous and isotropic media with local interaction Eq. (4) as will be subsequently shown in this paper, has the following form [3]

$$p_\alpha = A_0 \varepsilon_\alpha \tag{5}$$

If the strain energy per unit volume of the elastic medium with microstructure is denoted by $W = W(\varepsilon_\alpha, \mu_\alpha, \gamma_{\alpha i})$, then the stress power P is given by

$$P = \dot{W} = \sum_{\alpha=1}^{n} \left(p_\alpha \dot{\varepsilon}_\alpha + m_\alpha \dot{\mu}_\alpha + t_{\alpha i} \dot{\gamma}_{\alpha i} \right) \tag{6}$$

On the other hand, the time rate of change of W is

$$\dot{W} = \sum_{\alpha=1}^{n} \left(\frac{\partial W}{\partial \varepsilon_\alpha} \dot{\varepsilon}_\alpha + \frac{\partial W}{\partial \mu_\alpha} \dot{\mu}_\alpha + \frac{\partial W}{\partial \gamma_\alpha} \dot{\gamma}_{\alpha i} \right) \tag{7}$$

Comparing Eqs. (6) and (7), it is found

$$p_\alpha = \frac{\partial W}{\partial \varepsilon_\alpha}, m_\alpha = \frac{\partial W}{\partial \mu_\alpha}, t_{\alpha i} = \frac{\partial W}{\partial \gamma_\alpha} \tag{8}$$

For this medium, the functional

$$L\left[u, \phi\right] = \int_0^T \int_V (W - \frac{\rho}{2} |\dot{u}|^2 - F.u) dv dt - \int_0^T \int_S (T.u + M.\phi) dv dt \tag{9}$$

Is defined where T and M are the force and couple vectors per unit area of the surface S, respectively, F is the force per unit volume and ρ is the density. Taking the first variation of L in Eq. (9) yields

$$\left. \frac{d}{d\lambda} L\left[u + \lambda v, \phi + \lambda \theta\right] \right)_{\lambda=0} \tag{10}$$

where v and θ are arbitrary smooth functions with $v(R,0) = 0, \theta(R,0) = 0$ and setting it equal to zero and using Eq. (8), along with the definitions of the microstrains, yields the following results in terms of the microstresses [3]:

a) Conservation of linear momentum:

$$\sum_{\alpha=1}^{n} \sum_{x=1}^{M} (-1)^{x-1} \frac{\eta_\alpha^{x-1}}{x!} (\tau_\alpha^0 . \nabla)^x (t_{\alpha i} + p_{\alpha i}) + F_i = \rho \frac{\partial^2 u_i}{\partial t^2} \tag{11}$$

b) Conservation of moment of momentum:

$$\sum_{\alpha=1}^{n}\left[\varepsilon_{ijq}\tau_{\alpha j}^{0}t_{\alpha q}+\sum_{x=1}^{M}\left(-1\right)^{x-1}\frac{\eta_{\alpha}^{x-1}}{x!}\left(\tau_{\alpha}^{0}.\nabla\right)^{x}\left(m_{\alpha i}-\frac{1}{2}\eta_{\alpha}\varepsilon_{ijq}\tau_{\alpha j}^{0}t_{\alpha q}\right)\right]=0 \tag{12}$$

wherein $p_{\alpha i}=p_{\alpha}\tau_{\alpha i}^{0}$, $m_{\alpha i}=m_{\alpha}\tau_{\alpha i}^{0}$ and natural boundary conditions at the surface S as:

c) Force boundary conditions:

$$n_{k_r}\sum_{\alpha=1}^{n}\tau_{\alpha k_r}^{0}\sum_{x=1}^{M}(-1)^{x-1}\frac{\eta_{\alpha}^{x-1}}{x!}(\tau_{\alpha}^{0}.\nabla)^{x-r}(t_{\alpha i}+p_{\alpha i})=T_i\delta_{r1} \tag{13}$$

d) Couple boundary conditions:

$$n_{k_r}\sum_{\alpha=1}^{n}\tau_{\alpha k_r}^{0}\sum_{x=1}^{M}(-1)^{x-1}\frac{\eta_{\alpha}^{x-1}}{x!}(\tau_{\alpha}^{0}.\nabla)^{x-r}(m_{\alpha i}-\frac{1}{2}\eta_{\alpha}\varepsilon_{ijq}\tau_{\alpha j}^{0}t_{\alpha q})=-M_i\delta_{r1} \tag{14}$$

Here n denotes the outward unit normal to the surface S. The subscript $r=1,2,\dots,M-1$ if $M\geq 2$ and $r=1$ if $M=1$.However, r should be such that $r+1\leq x$ otherwise one has to take the product $\tau_{\alpha k_{r+1}}^{0}\tau_{\alpha k_{r+2}}^{0}\dots\tau_{\alpha k_{\chi}}^{0}=1$ and to ignore the differential operator in Eqs. (13) and (14) so that $\partial^{x-r}(...)=(\dots)$ [3].

The components of the surface force vector T and couple vector M are represented in the form [3]

$$T_i=\sigma_{ki}n_k\ ,M_i=M_{ki}n_k \tag{15}$$

where σ_{ki} and M_{ki} are components of the second order tensors of the force macrostresses T and the couple macrostresses M, respectively. By comparing Eq. (15) to Eqs. (13) and (14), it is easily found the natural connection between the microstresses and the macrostresses is found to be [3]:

$$\sigma_{\mathrm{ik}_1}^{(M)}=\sum_{\alpha=1}^{\mathrm{n}}\tau_{\alpha\mathrm{k}_1}^{0}\sum_{x=1}^{\mathrm{M}}(-1)^{x-1}\frac{\eta_{\alpha}^{x-1}}{x!}(\tau_{\alpha}^{0}.\nabla)^{x-1}(\mathrm{t}_{\alpha\mathrm{i}}+\mathrm{p}_{\alpha\mathrm{i}}) \tag{16}$$

$$M_{ik_1}^{(M)}=\sum_{\alpha=1}^{n}\tau_{\alpha k_1}^{0}\sum_{x=1}^{M}\left(-1\right)^{x-1}\frac{\eta_{\alpha}^{x-1}}{x!}\left(\tau_{\alpha}^{0}.\nabla\right)^{x-1}\left(m_{\alpha i}-\frac{1}{2}\eta_{\alpha}\varepsilon_{ijq}\tau_{\alpha j}^{0}t_{\alpha q}\right) \tag{17}$$

Superscript (M) refers to the generalized macrostresses which incorporate scale effects. Neglecting shear microstress and noting that $p_{\alpha i}=p_{\alpha}\tau_{\alpha i}^{0},\tau_{\alpha}^{0}=\tau_{\alpha j}^{0}e_j$, the relation between microstresses and macrostresses can be written as:

$$\sigma^{(M)}=\sum_{\alpha=1}^{n}\tau_{\alpha}^{0}\tau_{\alpha}^{0}\sum_{x=1}^{M}\frac{\left(-\eta_{\alpha}\right)^{x-1}}{x!}(\tau_{\alpha}^{0}.\nabla)^{x-1}p_{\alpha} \tag{18}$$

The three dimensional equation of motion in DM is given by [3]

$$\nabla.\sigma^{(M)}+F=\rho\frac{\partial^2 u}{\partial t^2} \tag{19}$$

where ρ, u and t are mass density, displacement vector and time, respectively.

Now the form of matrix $\left[A\right]$ in Eq. (4) containing elastic macroconstant for plane problem (two-dimensional) is obtained. For this reason, consider Fig. 3. According to Fig. 3, in the $x_1 - x_2$ plane there are only three doublets with equal angels between them. The solution for the scale-less condition can be calculated directly from the associated continuum mechanics problem for an isotropic material.

It is known from DM that, $\left[A\right]$ is a symmetric matrix of order 3 with the most general form [3]

$$\left[A\right] = \begin{bmatrix} a & b & b \\ b & a & b \\ b & b & a \end{bmatrix} \tag{20}$$

It is shown in Appendix A that the coefficients of matrix $\left[A\right]$ are independent of θ rendering the material isotropic. Furthermore the coefficients a and b in matrix $\left[A\right]$ for plane stress conditions are found to be [3]:

$$a = \frac{4}{9}\mu\frac{7\lambda+10\mu}{\lambda+2\mu}, b = \frac{4}{9}\mu\frac{\lambda-2\mu}{\lambda+2\mu} \tag{21}$$

One could use $b=0$ as a quantitative guide to the applicability of the simpler constitutive relations such as Eq. (5). If $\lambda = 2\mu$ (or $\nu = \frac{1}{3}$) in plane stress condition from Eq. (21), it is concluded that $b=0$ and

$$a = A_0 = \frac{8\mu}{3} = E \tag{22}$$

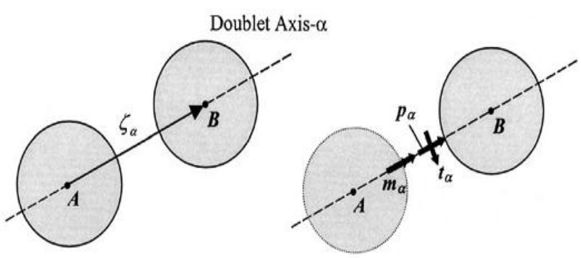

Fig.1
Doublet.

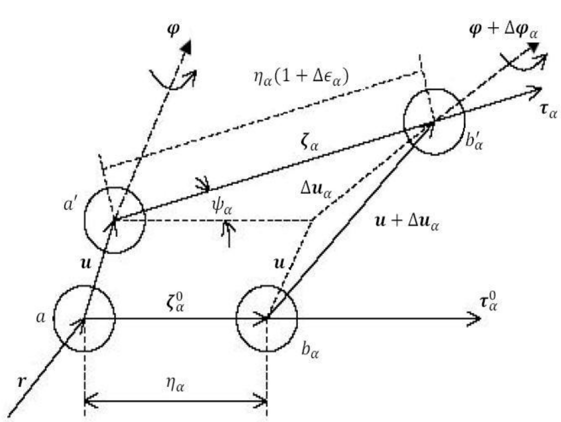

Fig.2
Translations of the doublet nodes $a \in A, b_o \in B_o$.

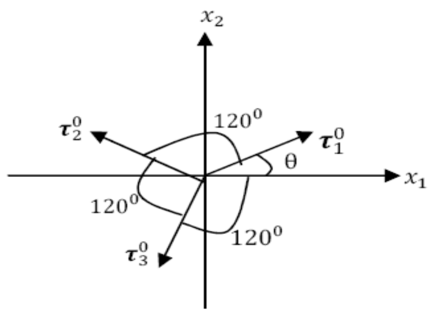

Fig.3
Scematic of atoms sort in nanostructure.

2.2 Comparison with the other theories

The classical theory of continuum mechanics is used to develop equations of motion wherein the small scale effects due to atomic scale of the lattice structures of CNTs are not taken into account. The effects of heterogeneity in nanostructures are not reasonably accounted for by direct application of classical continuum mechanics. Moreover, the length scales associated with nanotubes are often sufficiently small to call the applicability of classical continuum models into question [35]. Classical continuum mechanics modelling assumptions are conducive to erroneous results, when applied to material domains where the typical microstructural dimension is comparable with the structural ones [2].

Owning to nanoscale, it is difficult to set up controlled experiments to measure the properties of an individual carbon nanostructure. Also, atomistic methods like MD are costly and time consuming to implement particularly for large-scale systems [3].

Currently, various elegant modifications to continuum mechanics have been proposed to incorporate scale and microstructural features into the theory. The most important of these theories are nonlocal (gradient-type theory), molecular dynamics and Cosserat-type like couple stress theory. In this section, a brief comparison between these theories is presented.

The nonlocal theory is phenomenological in nature. That is, unlike DM the nonlocal theory is developed following a simplified pattern without considering a particular microstructure. Under such an approach, the parameters of the microstructure are not included in the mathematical model directly as in DM. The microstructural parameters enter the nonlocal theory indirectly because it is implicitly contained in the macrotensor of elasticity. Also, the total number of parameter in nonlocal and strain gradient theories in general is high and they implicitly contain the small scale effect but in DM, the small scale effect is contained explicitly.

Another important theory is MD which is based on the following assumptions: The first, any crystal is an infinite lattice structure and the second, the crystal obeys some devised periodic boundary conditions (PBC). It can be seen that MD in general, is incompatible with arbitrary boundary conditions [3].

DM is a new theory of elasticity stemming from consideration of the discrete microstructure of solids. Using DM, it is possible to determine the microstress distribution in granular media. If the doublet microstresses would be known, it is always possible to calculate the unknown macrotensors $\sigma_{ij}^{(M)}$ and $M_{ij}^{(M)}$. If $\sigma_{ij}^{(M)}$ and $M_{ij}^{(M)}$ would be known, in general, it is impossible to determine the doublet microstresses. This means that the doublet microstresses are more informative than the Cauchy $\sigma_{ij}^{(M)}$ and Cosserat $M_{ij}^{(M)}$ macrostresses and they provide, therefore, deeper insight into the mechanical behavior of solids. As such DM includes Cosserat models through couple microstresses M as in Eq. (17). It is noted that the couple-stress model is the simplest case of all the Cosserat models [36].

3 DM MODEL OF SLGSS

Specific applications of DM have been developed for two-dimensional problems with regular particle packing microstructures. One case that has been studied is the two-dimensional cubic hexagonal packing. This geometrical microstructure establishes three doublet axes at 120^0 angles as shown in Fig. 3. This structure is a nanostructure.

Now, consider a rectangular nanoplate having a length a, width b, density ρ, modulus of elasticity E, Poisson's ratio ν and uniform thickness h as shown in Fig. 4.

Classical plate theory is used in the subsequent formulation, according to which, the displacement field can be expressed as [30]:

$$u(x,y,z,t) = U(x,y,t) - z\frac{\partial w}{\partial x} \tag{23}$$

$$v\left(x,y,z,t\right) = V\left(x,y,t\right) - z\frac{\partial w}{\partial y} \tag{24}$$

$$w\left(x,y,z,t\right) = W\left(x,y,t\right) \tag{25}$$

where u,v and w are the displacement of the plate in x,y and z directions, respectively. U,V and V are the mid-plane displacements in x,y and z directions, respectively. The displacements of any arbitrary point can be determined using Eqs. (23)-(25).

The macrostrains in terms of displacement components can be written as [30]:

$$\varepsilon_{xx} = \frac{\partial U}{\partial x} - z\frac{\partial^2 W}{\partial x^2} \tag{26}$$

$$\varepsilon_{yy} = \frac{\partial V}{\partial y} - z\frac{\partial^2 W}{\partial y^2} \tag{27}$$

$$\gamma_{xy} = 2\varepsilon_{xy} = \frac{\partial U}{\partial y} + \frac{\partial V}{\partial x} - 2z\frac{\partial^2 W}{\partial x \partial y} \tag{28}$$

and other macrostrains are zero.

$$\varepsilon_{zz} = \gamma_{xz} = \gamma_{zy} = 0 \tag{29}$$

Expanding Eq. (19) in Cartesian coordinate in the absence of body forces in the *x* and *y* directions yields

$$\frac{\partial \sigma_{xx}^{(M)}}{\partial x} + \frac{\partial \sigma_{yx}^{(M)}}{\partial y} + \frac{\partial \sigma_{zx}^{(M)}}{\partial z} = \rho\frac{\partial^2 u}{\partial t^2} \tag{30}$$

$$\frac{\partial \sigma_{xy}^{(M)}}{\partial x} + \frac{\partial \sigma_{yy}^{(M)}}{\partial y} + \frac{\partial \sigma_{zy}^{(M)}}{\partial z} = \rho\frac{\partial^2 v}{\partial t^2} \tag{31}$$

$$\frac{\partial \sigma_{xz}^{(M)}}{\partial x} + \frac{\partial \sigma_{yz}^{(M)}}{\partial y} + \frac{\partial \sigma_{zz}^{(M)}}{\partial z} + f_z = \rho\frac{\partial^2 w}{\partial t^2} \tag{32}$$

Integrating Eq. (30) and Eq. (31) in the *z* direction and neglecting shear macrostresses $\sigma_{xz}^{(M)}, \sigma_{zy}^{(M)}$ in the upper and lower planes of the plate yields

$$\frac{\partial N_{xx}^{(M)}}{\partial x} + \frac{\partial N_{yx}^{(M)}}{\partial y} = \rho h\frac{\partial^2 U}{\partial t^2} \tag{33}$$

$$\frac{\partial N_{xy}^{(M)}}{\partial x}+\frac{\partial N_{yy}^{(M)}}{\partial y}=\rho h\frac{\partial^2 V}{\partial t^2} \tag{34}$$

where $N_{ij}^{(M)}$ are stresses resultants and defined as below:

$$\begin{bmatrix} N_{xx}^{(M)} \\ N_{yy}^{(M)} \\ N_{xy}^{(M)} \end{bmatrix}=\int_{-\frac{h}{2}}^{\frac{h}{2}}\begin{bmatrix} \sigma_{xx}^{(M)} \\ \sigma_{yy}^{(M)} \\ \sigma_{xy}^{(M)} \end{bmatrix}dz \tag{35}$$

Eqs. (33) and (34) are the equation of motions for plate in *x* and *y* directions, respectively.

Now, the equation of motion in the *z* direction is obtained. Differentiating Eqs. (30-31), and Eq. (32) with respect to x,y and *z* respectively and using Eqs. (26)-(28) and combining the results, it is found that

$$\frac{\partial^2\sigma_{xx}^{(M)}}{\partial x^2}+2\frac{\partial^2\sigma_{xy}^{(M)}}{\partial x\partial y}+\frac{\partial^2\sigma_{yy}^{(M)}}{\partial y^2}-\frac{\partial^2\sigma_{zz}^{(M)}}{\partial z^2}=\frac{\partial f_z}{\partial z}-\rho\frac{\partial^3 W}{\partial z\partial t^2}-\rho z\frac{\partial^4 W}{\partial x^2\partial t^2}-\rho z\frac{\partial^4 W}{\partial y^2\partial t^2} \tag{36}$$

Multiplication both side of Eq. (36) with respect to *z* and then integrating it with respect to *z* and neglecting $\sigma_{zz}^{(M)}$ due to the assumption of plane stress, it is found that

$$\frac{\partial^2 M_{xx}^{(M)}}{\partial x^2}+2\frac{\partial^2 M_{xy}^{(M)}}{\partial x\partial y}+\frac{\partial^2 M_{yy}^{(M)}}{\partial y^2}=q-\rho\frac{\partial^3 W}{\partial z\partial t^2}-\rho_0\frac{\partial^4 W}{\partial x^2\partial t^2}-\rho_2\frac{\partial^4 W}{\partial y^2\partial t^2} \tag{37}$$

where $q=\int_{-\frac{h}{2}}^{\frac{h}{2}} z\frac{\partial f_z}{\partial z}dz$ is the transverse force per unit area. Eq. (37) is the equation of motion for plate in the *z* direction wherein ρ_0 ,ρ_2 are defined by

$$\rho_0=\int_{-\frac{h}{2}}^{\frac{h}{2}}\rho dz\ ,\rho_2=\int_{-\frac{h}{2}}^{\frac{h}{2}}\rho z^2 dz \tag{38}$$

and $M_{ij}^{(M)}$ are moment resultants and defined as below:

$$\begin{bmatrix} M_{xx}^{(M)} \\ M_{yy}^{(M)} \\ M_{xy}^{(M)} \end{bmatrix}=\int_{-\frac{h}{2}}^{\frac{h}{2}}\begin{bmatrix} \sigma_{xx}^{(M)} \\ \sigma_{yy}^{(M)} \\ \sigma_{xy}^{(M)} \end{bmatrix}zdz \tag{39}$$

As is known, a SLGS is constructed from three doublets having equal lengths and angles. Now consider a Zigzag SLGS ($\theta=0$ in Fig. 3) which is shown in Fig. 5.

From Fig. 5, the director vectors in Cartesian coordinates are written as:

$$\tau_{11}^0 = 1\ ,\tau_{21}^0 = -cos60\ ,\tau_{31}^0 = -cos60 \tag{40}$$

$$\tau_{12}^0 = 0\ ,\tau_{22}^0 = cos30\ ,\tau_{32}^0 = -cos30 \tag{41}$$

$$\tau_{13}^0 = 0, \tau_{23}^0 = 0\ ,\tau_{33}^0 = 0 \tag{42}$$

It is further assumed that all doublets originating from a common node have the same magnitudes; i.e. $\eta_a = \eta\ (a = 1, 2, \ldots, n)$ and the interactions are purely axial (no shear or torsional microstresses is present). For local interaction in the plane, there will be two micromoduli *a,b* and the constitutive relationship between elongation microstress and microstrain is expressed by Eq. (4). If $\nu = \frac{1}{3}$, then matrix $\left[A\right]$ will be diagonal and there will be one micromodulus A_0 and the constitutive relationship between elongation microstress and microstrain is expressed by Eq. (5). In this paper Eq. (5) is used because volume of calculation with two micromodulus is overbearing.

If Eq. (3) is substituted into Eq. (5) and then the result is substituted into Eq. (18) and neglecting the terms with order $O(\eta^3)$ and higher, it can be found that

$$\sigma^{(M)} = \sum_{\alpha=1}^{n} \tau_\alpha^0 \tau_\alpha^0 \left\{ \tau_\alpha^0 . \left[\tau_\alpha^0 . \nabla u + \frac{1}{12} \eta^2 \left(\tau_\alpha^0 . \nabla \right) \left(\tau_\alpha^0 . \nabla \right) \left(\tau_\alpha^0 . \nabla u \right) \right] \right\} \tag{43}$$

This equation is the relation between macrostress and displacement with order $O(\eta^2)$. Noting that in Cartesian coordinate $\nabla = \frac{\partial}{\partial x_i} e_i$, Eq. (43) can be written as:

$$\sigma_{ij}^{(M)} = \sum_{\alpha=1}^{n} A_0 \tau_{\alpha i}^0 \tau_{\alpha j}^0 \tau_{\alpha m}^0 \tau_{\alpha n}^0 (\varepsilon_{mn} + \frac{1}{12} \eta^2 \tau_{\alpha t}^0 \tau_{\alpha s}^0 \frac{\partial^2 \varepsilon_{mn}}{\partial x_t \partial x_s}) \tag{44}$$

where ε_{mn} is the linear elastic macrostrain tensor defined by $\varepsilon_{mn} = \frac{1}{2}\left(\frac{\partial u_m}{\partial x_n} + \frac{\partial u_n}{\partial x_m} \right)$ in Cartesian coordinate.

It can be seen from Eq. (32) that nonlocal behavior enters into the problem through the constitutive relations. Expanding Eq. (44) and setting $i, j = x$ and using Eqs. (26)-(28) along with Eqs. (40)-(42), it is found that

$$\sigma_{xx}^{(M)} = A_0 \begin{bmatrix} -\frac{9}{8} z \frac{\partial^2 W}{\partial x^2} - \frac{3}{8} z \frac{\partial^2 W}{\partial y^2} - \frac{33}{384} \eta^2 z \frac{\partial^4 W}{\partial x^4} - \frac{18}{384} \eta^2 z \frac{\partial^4 W}{\partial x^2 \partial y^2} - \frac{9}{384} \eta^2 z \frac{\partial^4 W}{\partial y^4} + \\ \frac{9}{8} \frac{\partial U}{\partial x} + \frac{3}{8} \frac{\partial V}{\partial y} + \frac{9}{384} \eta^2 \left(\frac{\partial^3 U}{\partial x \partial y^2} + \frac{\partial^3 V}{\partial y \partial x^2} + \frac{\partial^3 V}{\partial y^3} \right) + \frac{33}{384} \eta^2 \frac{\partial^3 U}{\partial x^3} \end{bmatrix} \tag{45}$$

Similarly, the following relations for $\sigma_{yy}^{(M)}$, $\sigma_{xy}^{(M)}$ can be obtained

$$\sigma_{yy}^{(M)} = A_0 \begin{bmatrix} -\frac{9}{8} z \frac{\partial^2 W}{\partial y^2} - \frac{3}{8} z \frac{\partial^2 W}{\partial x^2} - \frac{27}{384} \eta^2 z \frac{\partial^4 W}{\partial y^4} - \frac{36}{384} \eta^2 z \frac{\partial^4 W}{\partial x^2 \partial y^2} - \frac{3}{384} \eta^2 z \frac{\partial^4 W}{\partial x^4} + \\ \frac{9}{8} \frac{\partial V}{\partial y} + \frac{3}{8} \frac{\partial U}{\partial x} + \frac{27}{384} \eta^2 \frac{\partial^3 V}{\partial y^3} + \frac{18}{384} \eta^2 \left(\frac{\partial^3 U}{\partial x \partial y^2} + \frac{\partial^3 V}{\partial y \partial x^2} \right) + \frac{3}{384} \eta^2 \frac{\partial^3 U}{\partial x^3} \end{bmatrix} \tag{46}$$

$$\sigma_{xy}^{(M)}=A_0\left[\begin{array}{l}-\frac{3}{4}z\frac{\partial^2 W}{\partial x\partial y}-\frac{27}{384}\eta^2 z\frac{\partial^4 W}{\partial x\partial y^3}-\frac{9}{384}\eta^2 z\frac{\partial^4 W}{\partial y\partial x^3}+\frac{3}{2}\left(\frac{\partial U}{\partial y}+\frac{\partial V}{\partial x}\right)+\\ \frac{27}{384}\eta^2\left(\frac{\partial^3 U}{\partial y^3}+\frac{\partial^3 V}{\partial x\partial y^2}\right)+\frac{9}{384}\eta^2\left(\frac{\partial^3 U}{\partial y\partial x^2}+\frac{\partial^3 V}{\partial x^3}\right)\end{array}\right] \tag{47}$$

Because the plate is in plane stress condition from Eq. (22) for one micromodulus, it is found that $\nu=\frac{1}{3}$ and $A_0=E$.

As is known, the flexural rigidity of plate is obtained from $D=\frac{Eh^3}{12(1-\nu^2)}$. For $\nu=\frac{1}{3}$, it may be concluded that $\frac{h^3}{12}E=\frac{8}{9}D$. If Eqs. (45)-(47) are substituted into Eq. (39) and integrations are performed, the following equations for moments can be obtained

$$M_{xx}^{(M)}=\frac{8}{9}D\left(-\frac{9}{8}\frac{\partial^2 W}{\partial x^2}-\frac{3}{8}\frac{\partial^2 W}{\partial y^2}-\frac{33}{384}\eta^2\frac{\partial^4 W}{\partial x^4}-\frac{18}{384}\eta^2\frac{\partial^4 W}{\partial x^2\partial y^2}-\frac{9}{384}\eta^2\frac{\partial^4 W}{\partial y^4}\right) \tag{48}$$

$$M_{yy}^{(M)}=\frac{8}{9}D\left(-\frac{9}{8}\frac{\partial^2 W}{\partial y^2}-\frac{3}{8}\frac{\partial^2 W}{\partial x^2}-\frac{27}{384}\eta^2\frac{\partial^4 W}{\partial y^4}-\frac{36}{384}\eta^2\frac{\partial^4 W}{\partial x^2\partial y^2}-\frac{3}{384}\eta^2\frac{\partial^4 W}{\partial x^4}\right) \tag{49}$$

$$M_{xy}^{(M)}=\frac{8}{9}D\left(-\frac{6}{8}\frac{\partial^2 W}{\partial x\partial y}-\frac{27}{384}\eta^2\frac{\partial^4 W}{\partial x\partial y^3}-\frac{9}{384}\eta^2\frac{\partial^4 W}{\partial y\partial x^3}\right) \tag{50}$$

If Eqs. (48)-(50) are substituted into the Eq. (37), the following equation of motion in term of W can be obtained

$$-\frac{8}{9}D\left(\begin{array}{l}\frac{9}{8}\frac{\partial^4 W}{\partial y^4}+\frac{18}{8}\frac{\partial^4 W}{\partial x^2\partial y^2}+\frac{9}{8}\frac{\partial^4 W}{\partial x^4}+\frac{33}{384}\eta^2\frac{\partial^6 W}{\partial x^6}+\\ \frac{27}{384}\eta^2\frac{\partial^6 W}{\partial y^6}+\frac{39}{384}\eta^2\frac{\partial^6 W}{\partial x^4\partial y^2}+\frac{99}{384}\eta^2\frac{\partial^6 W}{\partial y^4\partial x^2}\end{array}\right)+q=\rho_0\frac{\partial^2 W}{\partial t^2}-\rho_2\left(\frac{\partial^4 W}{\partial x^2\partial t^2}+\frac{\partial^4 W}{\partial y^2\partial t^2}\right) \tag{51}$$

Eq. (51) is a sixth-order governing equation for the lateral displacement of the nanoplate. However, the governing equation derived from the doublet mechanics principles turns out to be an infinite order differential equation in terms of η. Since it is almost impossible to solve the infinite order differential equation, only terms of order $M=2$ and lower in the infinite series in Eqs. (3) and (18) are retained. For the general case where scale is present, Eq. (51) is the basic equation of motion incorporating the scale effect.

It is assumed that the boundaries forces of the plate are independent to scale. Then the displacement fields can be written by the following equation [3]

$$W=W_0+\eta^2 W_2 \tag{52}$$

Suppose that the boundaries of the plate are simply supported. Then it can be concluded that

$$W(x,y,t)=M_{xx}^{(M)}(x,y,t)=0\; at\; x=0,a \tag{53}$$

$$W(x,y,t)=M_{yy}^{(M)}(x,y,t)=0\; at\; y=0,b \tag{54}$$

Substituting Eqs. (53), (54) in to Eq. (52) yields

$$W_0\left(x,y,t\right)=M_{xx}^{(M)}\left(x,y,t\right)=0\,at\,x=0,a \tag{55}$$

$$W_0\left(x,y,t\right)=M_{yy}^{(M)}\left(x,y,t\right)=0\,at\,y=0,b \tag{56}$$

$$W_2\left(x,y,t\right)=M_{xx}^{(M)}\left(x,y,t\right)=0\,at\,x=0,a \tag{57}$$

$$W_2\left(x,y,t\right)=M_{yy}^{(M)}\left(x,y,t\right)=0\,at\,y=0,b \tag{58}$$

To find the frequency of lateral vibration of nanoplate, the following solution for the lateral vibrations of nanoplate is considered as:

$$W=(A_{mn}+\eta^2 B_{mn}).sin\frac{m\pi}{a}x.sin\frac{n\pi}{b}y.sin\omega_{mn}^{(\eta)}t \tag{59}$$

where A_{mn} and B_{mn} are the amplitudes of lateral vibration, $\omega_{mn}^{(\eta)}$ is the frequency of lateral vibration, *m* and *n* are half wave numbers in the x,y directions, respectively.

Substituting Eq. (59) into Eq. (51), $\left(\omega_{mn}^{(\eta)}\right)^2$ can be obtained as follows:

$$\left(\omega_{mn}^{(\eta)}\right)^2=\frac{D}{\rho_0+\rho_2\left[\left(\frac{m\pi}{a}\right)^2+\left(\frac{n\pi}{b}\right)^2\right]}\left\{\begin{array}{l}\left(\frac{n\pi}{b}\right)^4+2\left(\frac{n\pi}{b}\right)^2\left(\frac{m\pi}{a}\right)^2+\left(\frac{m\pi}{a}\right)^4+\\-\frac{\eta^2}{144}\left[\begin{array}{l}11\left(\frac{m\pi}{a}\right)^6+9\left(\frac{n\pi}{b}\right)^6+\\13\left(\frac{n\pi}{b}\right)^2\left(\frac{m\pi}{a}\right)^4+33\left(\frac{n\pi}{b}\right)^4\left(\frac{m\pi}{a}\right)^2\end{array}\right]\end{array}\right\} \tag{60}$$

which is the frequency equation of lateral vibration of the Zigzag nanoplate with scale effect.

For an Armchair nanoplate, similar calculations yields equation of motion and natural frequency as below

$$\begin{aligned}&D\left[\frac{\partial^4 w}{\partial x^4}+\frac{\partial^4 W}{\partial y^4}+2\frac{\partial^4 W}{\partial x^2\partial y^2}+\frac{1}{16}\eta^2\frac{\partial^6 W}{\partial x^6}+\frac{1}{216}\eta^2\frac{\partial^6 W}{\partial y^6}+\frac{11}{48}\eta^2\frac{\partial^6 W}{\partial x^4\partial y^2}+\frac{11}{144}\eta^2\frac{\partial^6 W}{\partial x^2\partial y^4}\right]\\&=\left(\omega_{mn}^{(\eta)}\right)^2\left\{\rho_0+\rho_2\left[\left(\frac{m\pi}{a}\right)^2+\left(\frac{n\pi}{b}\right)^2\right]\right\}\end{aligned} \tag{61}$$

$$\left(\omega_{mn}^{(\eta)}\right)^2=\frac{D}{\rho_0+\rho_2\left[\left(\frac{m\pi}{a}\right)^2+\left(\frac{n\pi}{b}\right)^2\right]}\left\{\begin{array}{l}\left(\frac{m\pi}{a}\right)^4+\left(\frac{n\pi}{b}\right)^4+2\left(\frac{n\pi}{b}\right)^2\left(\frac{m\pi}{a}\right)^2+\\-\frac{\eta^2}{432}\left[\begin{array}{l}27\left(\frac{m\pi}{a}\right)^6+34\left(\frac{n\pi}{b}\right)^6+99\left(\frac{n\pi}{b}\right)^2\left(\frac{m\pi}{a}\right)^4\\+33\left(\frac{n\pi}{b}\right)^4\left(\frac{m\pi}{a}\right)^2\end{array}\right]\end{array}\right\} \tag{62}$$

In the scale less condition where $\eta = 0$, from Eq. (60) and/or Eq. (62), it is found that

$$\omega_{mn}^2 = \frac{D\left[\left(\frac{n\pi}{b}\right)^4 + 2\left(\frac{n\pi}{b}\right)^2\left(\frac{m\pi}{a}\right)^2 + \left(\frac{m\pi}{a}\right)^4\right]}{\rho_0 + \rho_2\left[\left(\frac{m\pi}{a}\right)^2 + \left(\frac{n\pi}{b}\right)^2\right]} \tag{63}$$

which is in exact in agreement with frequency obtained in [23] for lateral vibration of simply supported SLGSs in scale-less condition.

It is evident from Eq. (60) and Eqs. (62), (63) that using a continuum plate model in the frequency analysis of a nanoplate can cause an overestimate. However as the dimensions of the plate increases, the difference between natural frequency of lateral vibration with and without scale parameter becomes smaller and the frequencies of the two models have a good agreement. It is also seen that the presence of the nanoscale η decreases the natural frequency. But as the dimensions of the plate increase, the effect of scale decreases.

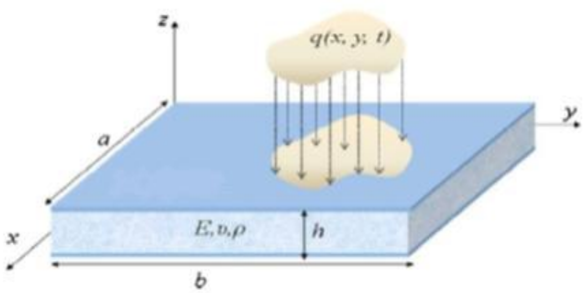

Fig.4
Three doublets with equal angle 120^0 between them.

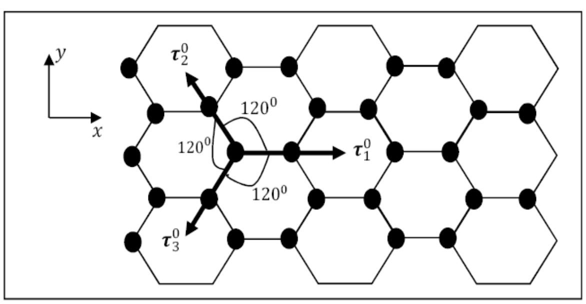

Fig.5
Schematic of atoms sort in a Zigzag SLGS.

4 RESULTS AND DISCUSSION

Comparison between the results obtained in this work and the available MD and nonlocal results [31] for Zigzag and Armchair SLGSs are provided below.

Tables 1. and 2 show the natural frequencies for lateral vibration mode for 8 different SLGSs in comparison with the available MD and nonlocal results for Zigzag and Armchair nanoplates, respectively. As mentioned before the underlying microstructural parameter enters implicitly into the analysis of frequency in the nonlocal theory whereas in Eqs. (60) and (62) the scale parameter η is explicitly shown.

The nanoplates are square and the first columns show the length size of square nanoplates and the next three columns are the results. Throughout the paper, the material properties of SLGSs have been considered as: Young's modulus $E = 1TPa$, mass density $\rho = 2250\frac{kg}{m^3}$, plate thickness $h = 0.34nm$ and Poisson's ratio $\nu = 0.16$ [31]. In the DM model, the scale parameter used is the carbon-carbon bound length which is equal to $\eta = 0.142nm$ [37].

From Table. 1 and Table. 2, it could be concluded that the present paper's prediction of the natural frequencies for lateral vibration mode of different SLGSs is in good agreement with the available MD and non local results. In this section, numerical results are given for different vibration modes. The free vibration frequency ratio is defined as follows:

$$Frequency\,ratio = \frac{natural\ frequency\ calculated\ using\ DM\ theory}{natural\ frequency\ calculated\ using\ local\ (continuum)\ theory}$$

Table 1
Natural frequencies (*THz*) of simply-supported Zigzag SLGSs for different Side Length (*nm*).

Side Length (nm)	MD [31]	Nonlocal [31]	DM (present work)
15	0.0273881	0.0282888	0.02925433990
20	0.0157525	0.0164593	0.01645897156
25	0.0099840	0.1070850	0.01053475096
30	0.0070655	0.0075049	0.00731618003
35	0.0052982	0.0055447	0.00537532137
40	0.0040985	0.0042608	0.00411556425
45	0.0032609	0.0033751	0.00325184927
50	0.0026194	0.0027388	0.00263402422

Table 2
Natural frequencies (*THz*) of simply-supported Armchair SLGSs for different Side Length (*nm*).

Side Length (nm)	MD [31]	Nonlocal [31]	DM (present work)
15	0.0277928	0.0284945	0.02925437733
20	0.0158141	0.0165309	0.01645898341
25	0.0099975	0.0107393	0.01053475581
30	0.0070712	0.0075201	0.00731618237
35	0.0052993	0.0055531	0.00537532263
40	0.0041017	0.0042657	0.00411556499
45	0.0032614	0.0033782	0.00325184973
50	0.0026197	0.0027408	0.00263402452

The numerical results of free vibrating nanoplates for lateral mode are given in graphical form in Figs. 6 and 7. In Fig. 6 variation of frequency ratio parameters with plate side length is given for different vibration mode for Zigzag and Armchair nanoplates for simply supported boundary conditions when the scale parameter $\eta = 0.142\,nm$. According to these figures, as the dimensions of nanoplate increases, the frequency ratio increases. This increase is more apparent for higher modes and it can be seen that frequency ratio for Zigzag nanoplate is slightly more than the Armchair one. Since scale effects are more apparent for smaller wave lengths, after a certain plate length, frequency ratios approach a certain value.

Variation of frequency ratio of nanoplates as a function of scale effect for different half mode numbers for a square plate with 20 *nm* length is plotted in Fig. 7. According to Fig. 7 frequency ratio is decreasing with increase in η. This is more apparent for higher modes of vibration.

In Fig. 8, the variation of fundamental frequency ratio ($m = n = 1$) of rectangular-nanoplates as a function of scale parameter for different aspect ratios ($Aspect\,Ratio\ (A.R.) = \frac{b}{a}$) is plotted for Zigzag and Armchair SLGSs for $a = 30\,nm$. According to this figure, frequency ratio increases with increase in η for all aspect ratios. This increase is more apparent for lower aspect ratios. On the other hand, the effect of scale parameter for lower aspect ratios is more pronounced.

From Eqs. (60),(62) and (63) and the above figures, it can be concluded that vibration characteristic of the nanoplates depends on the size of the plate, half wave modes of vibration and scale parameter. Also the effect of the scale parameter is more apparent in higher modes of vibration and lower dimensions of the tube. It is also seen that the presence of the scale parameter η decreases the natural frequency. However, as the dimensions of the plate increase, the effect of scale parameter decreases.

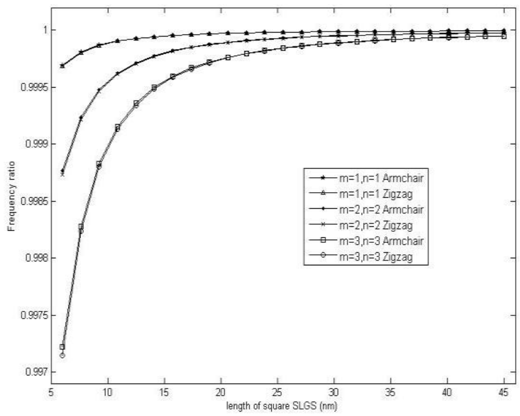

Fig.6
Variation of frequency ratios with plate side length for different vibration modes.

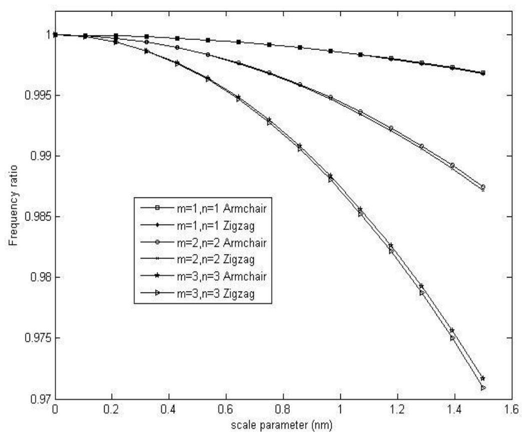

Fig.7
Variation of frequency ratio with length scale($a = b = 20nm$) for different vibration modes.

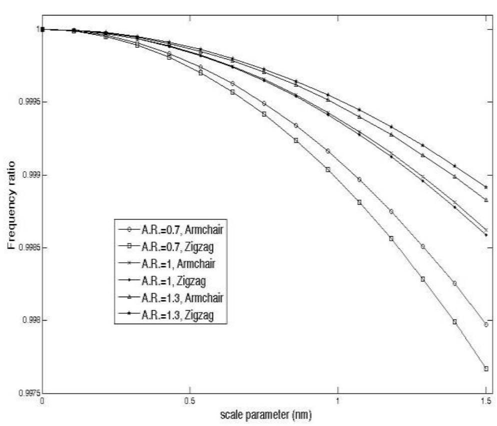

Fig.8
Variation of frequency ratio with scale parameter ($a = 30nm$) for different aspect ratios.

5 CONCLUSIONS

A new theory called DM has been employed to model the lateral vibration of simply supported SLGSs. The governing equation of motion in lateral direction was obtained in terms of lateral displacement and was solved analytically to obtain a closed form expression for the natural frequency of such SLGSs. Four major points are concluded in this study. Firstly, the length scale effect decreases natural frequency of the SLGSs in lateral mode vibration based on the DM model presented here. In other words, the nanoplate stiffness is lessened in comparison with the prediction of the classical continuum theory. Secondly, for a nanoplate with sufficiently large dimensions, the nanoscale effect becomes insignificant and thus the governing equation can be reduced to the classical equation. In this case both DM and classical continuum theory are in good agreement. Thirdly, frequency ratio for Zigzag nanoplate is slightly more than the Armchair one. Lastly, frequency ratio increases with increase in scale parameter for all aspect ratios. This is more apparent for lower aspect ratios.

APPENDIX A

A plane problem with three doublets in the plane is considered under scale-less condition ($M=1$). From Eq. (18), the relation between macrostresses and microstresses may be written as [3]:

$$\{\sigma\}=[M]\{p\} \tag{A.1}$$

where

$$\{\sigma\}=\begin{bmatrix}\sigma_{xx}\\ \sigma_{yy}\\ \sigma_{xy}\end{bmatrix},[M]=\begin{bmatrix}\left(\tau_{11}^{0}\right)^{2} & \left(\tau_{21}^{0}\right)^{2} & \left(\tau_{31}^{0}\right)^{2}\\ \left(\tau_{12}^{0}\right)^{2} & \left(\tau_{22}^{0}\right)^{2} & \left(\tau_{32}^{0}\right)^{2}\\ \tau_{11}^{0}\tau_{12}^{0} & \tau_{21}^{0}\tau_{22}^{0} & \tau_{31}^{0}\tau_{32}^{0}\end{bmatrix},\{p\}=\begin{bmatrix}p_1\\ p_2\\ p_3\end{bmatrix} \tag{A.2}$$

In addition, it may be shown that [3]

$$\{\varepsilon\}=[M]^{T}[\boldsymbol{\varepsilon}] \tag{A.3}$$

where,

$$\{\varepsilon\}=\begin{bmatrix}\varepsilon_{xx}\\ \varepsilon_{yy}\\ \varepsilon_{xy}\end{bmatrix},\{\varepsilon\}=\begin{bmatrix}\varepsilon_1\\ \varepsilon_2\\ \varepsilon_3\end{bmatrix} \tag{A.4}$$

From the classical (continuum mechanics) theory, the relation between macrostresses and macrostrains is given by

$$\{\sigma\}=[C]\{\varepsilon\} \tag{A.5}$$

where $[C]$ is the tensor of elasticity written below under plane stress and plane strain conditions as Eq. (A.6) and Eq. (A.7), respectively

$$[C]=\begin{bmatrix}\lambda+2\mu & \lambda & 0\\ \lambda & \lambda+2\mu & 0\\ 0 & 0 & \mu\end{bmatrix} \tag{A.6}$$

$$[\boldsymbol{C}]=\begin{bmatrix} 4\mu\left(\dfrac{\lambda+\mu}{\lambda+2\mu}\right) & \dfrac{2\mu\lambda}{\lambda+2\mu} & 0 \\ \dfrac{2\mu\lambda}{\lambda+2\mu} & 4\mu\left(\dfrac{\lambda+\mu}{\lambda+2\mu}\right) & 0 \\ 0 & 0 & \mu \end{bmatrix} \tag{A.7}$$

where λ ,μ are Lame constants which can be written in terms of the Young modulus E, Poisson ratio ν and shear modulus G as:

$$\lambda=\frac{\nu E}{(1+\nu)(1-2\nu)}\ ,\mu=G=\frac{E}{2(1+\nu)} \tag{A.8}$$

From Eqs. (4), (A.1), (A.3), (A.5), it may be concluded that

$$[C]=[M][A][M]^T \tag{A.9}$$

In the isotropic case, from the second part of Eq. (A.2), matrix $[M]$ can be written as:

$$[M]=\begin{bmatrix} cos^2\theta & cos^2(\theta+60) & cos^2(\theta+120) \\ sin^2\theta & sin^2(\theta+60) & sin^2(\theta+120) \\ sin\theta cos\theta & sin(\theta+60)cos(\theta+60) & sin(\theta+120)cos(\theta+120) \end{bmatrix} \tag{A.10}$$

It is shown below that for any angle θ, the coefficients of $[A]$ are independent of θ under plane stress and plane strain conditions thereby rendering the material isotropic. To this end, coefficient C_{11} in Eq. (A.9), is determined using Eq. (20) and Eq. (A.10) to be

$$\begin{aligned} &acos^4(\theta)+bcos^2(\theta)cos^2(\theta+120)+bcos^2(\theta)cos^2(\theta+240)+bcos^2(\theta)cos^2(\theta+120)+ \\ &acos^4(\theta+120)+bcos^2(\theta+120)cos^2(\theta+240)+bcos^2(\theta)cos^2(\theta+240)+ \\ &acos^4(\theta+240)+bcos^2(\theta+120)cos^2(\theta+240) \end{aligned} \tag{A.11}$$

Eq. (A.11) can be simplified to obtain

$$\begin{aligned} &a\left[cos^4(\theta)+cos^4(\theta+120)+cos^4(\theta+240)\right]+ \\ &2b\left[cos^2(\theta)cos^2(\theta+120)+cos^2(\theta)cos^2(\theta+240)+cos^2(\theta+120)cos^2(\theta+240)\right] \end{aligned} \tag{A.12}$$

The following trigonometric identities

$$cos(\theta+120)=cos(\theta)cos(120)-sin(\theta)sin(120)=\frac{1}{2}\left[-cos(\theta)-\sqrt{3}sin(\theta)\right] \tag{A.13}$$

$$cos(\theta+240)=cos(\theta)cos(240)-sin(\theta)sin(240)=\frac{1}{2}\left[-cos(\theta)+\sqrt{3}sin(\theta)\right] \tag{A.14}$$

May be used in Eq. (A.12) to yield

$$
\begin{aligned}
&a\left\{\begin{array}{l}
cos^4(\theta)+\frac{1}{16}\left[cos^2(\theta)+3sin^2(\theta)-2\sqrt{3}cos(\theta)sin(\theta)\right]^2+\\
\frac{1}{16}\left[cos^2(\theta)+3sin^2(\theta)+2\sqrt{3}cos(\theta)sin(\theta)\right]^2
\end{array}\right\}+\\
&b\left\{\begin{array}{l}
\frac{1}{2}cos^2(\theta)\left[cos^2(\theta)+3sin^2(\theta)-2\sqrt{3}cos(\theta)sin(\theta)\right]+\\
\frac{1}{2}cos^2(\theta)\left[cos^2(\theta)+3sin^2(\theta)+2\sqrt{3}cos(\theta)sin(\theta)\right]+\\
\frac{1}{8}\left[cos^2(\theta)+3sin^2(\theta)-2\sqrt{3}cos(\theta)sin(\theta)\right]\left[cos^2(\theta)+3sin^2(\theta)+2\sqrt{3}cos(\theta)sin(\theta)\right]
\end{array}\right\}
\end{aligned}
\tag{A.15}
$$

Making some simplifications, Eq. (A.15) can be reduced to

$$
\begin{aligned}
&\frac{9}{8}a\left[cos^4(\theta)+sin^4(\theta)+2cos^2(\theta)sin^2(\theta)\right]+\frac{9}{8}b\left[cos^4(\theta)+sin^4(\theta)+2cos^2(\theta)sin^2(\theta)\right]\\
&=\frac{9}{8}a\left[cos^2(\theta)+sin^2(\theta)\right]^2+\frac{9}{8}b\left[cos^2(\theta)+sin^2(\theta)\right]^2=\frac{9}{8}(a+b)
\end{aligned}
\tag{A.16}
$$

Similar calculations for C_{12}, C_{21} and C_{22} yield

$$C_{12}=\frac{3}{8}a+\frac{3}{4}b \tag{A.17}$$

$$C_{21}=\frac{3}{8}a+\frac{3}{4}b \tag{A.18}$$

$$C_{22}=\frac{9}{8}(a+b) \tag{A.19}$$

Therefore, Eqs. (A.16)- (A.19) may be used to write the elasticity tensor $[C]$ as:

$$[C]=\begin{bmatrix} C_{11} & C_{12}\\ C_{21} & C_{22}\end{bmatrix}=\frac{3}{4}\begin{bmatrix}\frac{3}{2}(a+b) & \frac{1}{2}a+b\\ \frac{1}{2}a+b & \frac{3}{2}(a+b)\end{bmatrix} \tag{A.20}$$

As is well known, the tensor $[C]$ in plane stress and plane stress conditions may be written with Eq. (A.20) and Eq. (A.21), respectively [3].

$$[C]=\begin{bmatrix} 4\mu\left(\frac{\lambda+\mu}{\lambda+2\mu}\right) & \frac{2\mu\lambda}{\lambda+2\mu} & 0\\ \frac{2\mu\lambda}{\lambda+2\mu} & 4\mu\left(\frac{\lambda+\mu}{\lambda+2\mu}\right) & 0\\ 0 & 0 & \mu\end{bmatrix} \tag{A.21}$$

$$[C]=\begin{bmatrix}\lambda+2\mu & \lambda & 0\\ \lambda & \lambda+2\mu & 0\\ 0 & 0 & \mu\end{bmatrix} \tag{A.22}$$

where μ and λ are given by

$$\lambda=\frac{\nu E}{(1+\nu)(1-2\nu)} \tag{A.23}$$

$$\mu=G=\frac{E}{2(1+\nu)} \tag{A.24}$$

If Eq. (A.20) and Eq. (A.21) for plane stress and Eq. (A.20) and Eq. (A.22) for plane strain conditions are considered, the coefficients *a* and *b* are determined to be

For plane stress:

$$a=\frac{4}{9}\mu\frac{7\lambda+10\mu}{\lambda+2\mu}\ ,b=\frac{4}{9}\mu\frac{\lambda-2\mu}{\lambda+2\mu} \tag{A.25}$$

For plane strain:

$$a=\frac{4}{9}(\lambda+5\mu)\ ,b=\frac{4}{9}(\lambda-\mu) \tag{A.26}$$

As it is seen, coefficients *a* and *b* and therefore tensor $[A]$ are independent of θ. For $b=0$, matrix $[A]$ is diagonal and this happens when $\lambda=2\mu$ $(\nu=\frac{1}{3})$ for plane stress and $\lambda=\mu$ $(\nu=\frac{1}{4})$ for plane strain. In this case, the coefficient *a* in plane stress and plane stress conditions may be written with Eq. (A.20) and Eq. (A.21), respectively.

$$a=\frac{4}{9}\mu\frac{7\lambda+10\mu}{\lambda+2\mu} \tag{A.27}$$

$$a=\frac{8}{3}\mu=E \tag{A.28}$$

REFERENCES

[1] Granik V.T., 1997, Microstructural mechanics of granular media, Technique Report IM/MGU 78-241, Institute of Mechanics of Moscow State University, in Russian.

[2] Granik V.T., Ferrari M., 1993, Microstructural mechanics of granular media, *Mechanics of Materials* **15**: 301-322.

[3] Ferrari M., Granik V.T., Imam A., Nadeau J., 1997, *Advances in Doublet Mechanics*, Springer, Berlin.

[4] Kojic M., Vlastelica I., Decuzzi P., Granik V.T., Ferrari M., 2011, A finite element formulation for the doublet mechanics modeling of microstructural materials, *Computer Methods in Applied Mechanics and Engineering* **200**: 1446-1454.

[5] Xin J., Zhou L.X., Ru W.J., 2009, Ultrasound attenuation in biological tissue predicted by the modified doublet mechanics model, *Chinese Physics Letters* **26**(7): 074301.1-074301.4.

[6] Ferrari M., 2000, Nanomechanics, and biomedical nanomechanics: Eshelby's inclusion and inhomogeneity problems at the discrete continuum interface, *Biomedical Microdevices* **2**(4): 273-281.

[7] Gentile F., Sakamoto J., Righetti R., Decuzzi P., Ferrari M., 2011, A doublet mechanics model for the ultrasound characterization of malignant tissues, *Journal of Biomedical Science and Engineering* **4**: 362-374.
[8] Lin S.S., Shen Y.C., 2005, Stress fields of a half-plane caused by moving loads-resolved using doublet mechanics, *Soil Dynamics and Earthquake Engineering* **25**: 893-904.
[9] Sadd M.H., Dai Q., 2005, A comparison of micro-mechanical modeling of asphalt materials using finite elements and doublet mechanics, *Mechanics of Materials* **37**: 641-662.
[10] Fang J.Y., Jue Z., Jing F., Ferrari M., 2004, Dispersion analysis of wave propagation in cubic-Tetrahedral assembly by doublet mechanics, *Chinese Physics Letters* **21**(8): 1562-1565.
[11] Sadd M. H., 2005, *Elasticity Theory Applications, and Numeric*, Elsevier Butterworth-Heinemann, Burlington.
[12] Eringen A.C., 1972, Nonlocal Polar Elastic Continua, *International Journal of Engineering Science* **10**: l-16.
[13] Iijima S., 1991, Helical microtubes of graphitic carbon, *Nature* **354**: 56-58.
[14] Katsnelsona M.I., Novoselov K.S., 2007, Graphene: New bridge between condensed matter physics and quantum electrodynamics, *Solid State Communications* **143**: 3-13.
[15] Heersche H.B., Herrero P.J., Oostinga J.B., Vandersypen L.M.K., Morpurgo A.F., 2007, Induced superconductivity in graphene, *Solid State Communications* **143**: 72-76.
[16] Stankovich S., Dikin D.A., Piner R.D., Kohlhaas K.A., Kleinhammes A., Jia Y., Wu Y., Nguyen S.T., Ruoff R.S., 2007, Synthesis of graphene-based nanosheets via chemical reduction of exfoliated graphite oxide, *Carbon* **45**: 1558-1565.
[17] Danesh M., Farajpour A., Mohammadi M., 2012, Axial vibration analysis of a tapered nanorod based on nonlocal elasticity theory and differential quadrature method, *Mechanics Research Communications* **39**: 23-27.
[18] Wang Q, C Wang M., 2007, The constitutive relation and small scale parameter of nonlocal continuum mechanics for modelling carbon nanotubes, *Nanotechnology* **18**: 075702.1-075702.4.
[19] Ghannadpour S.A.M., Mohammadi B., Fazilati J., 2013, Bending, buckling and vibration problems of nonlocal Euler beams using Ritz method, *Composite Structures* **96**: 584-589.
[20] Malekzadeh P., Mohebpour S. R., Heydarpour Y., 2012, Nonlocal effect on the free vibration of short nanotubes embedded in an elastic medium, *Acta Mechanica* **223**: 1341-1350.
[21] Stankovich S., Piner R.D, Nguyen S.T., Ruoff R.S., 2006, Synthesis and exfoliation of isocyanate-treated graphene oxide nanoplatelets, *Carbon* **44**: 3342-3347.
[22] Wang J., Tian M., He X., Tang Z., 2014, Free vibration analysis of single-layered graphene sheets based on a continuum model, *Applied Physics Frontier* **2**(1): 1-7.
[23] Rao S.S., 2007, *Vibration of Continuous Systems*, John Wiley and Sons, New Jersey.
[24] Green A.E., Zerna W., 1992, *Theoretical Elasticity*, Dover publications, New York.
[25] Reddy J.N., 2010, Non-local nonlinear formulations for bending of classical and shear deformation theories of beams and plates *International Journal of Engineering Science* **48**(11): 1507-1518.
[26] Aghababaei R., Reddy J.N., 2009, Nonlocal third-order shear deformation plate theory with application to bending and vibration of plates, *Journal of Sound and Vibration* **326**(1-2): 277-289.
[27] Farajpour A., Mohammadi M., Shahidi A.R., Mahzoon M., 2011, Axisymmetric buckling of the circular graphene sheets with the nonlocal continuum plate model, *Physica E: Low-dimensional Systems and Nanostructures* **43**(10): 1820-1825.
[28] Pradhan S.C., Phadikar J. K., 2009, Nonlocal elasticity theory for vibration of nanoplates, *Journal of Sound and Vibration* **325**: 206-223.
[29] Alibeigloo A., 2011, Free vibration analysis of nano-plate using three-dimensional theory of elasticity, *Acta Mechanica* **222**: 149-159.
[30] Aksencer T., Aydogdu M., 2011, Levy type solution method for vibration and buckling of nanoplates using nonlocal elasticity theory, *Physica E* **43**: 954-959.
[31] Ansari R., Sahmani S., Arash B., 2010, Nonlocal plate model for free vibrations of single-layered graphene sheets, *Physics Letters A* **375**: 53-62.
[32] Jalali S.K., Rastgoo A., Eshraghi I., 2011, Large amplitude vibration of imperfect shear deformable nano-plates using non-local theory, *Journal of Solid Mechanics* **3**(1): 64-73.
[33] Rouhi S., Ansari R., 2012, Atomistic finite element model for axial buckling and vibration analysis of single-layered graphene sheets, *Physica E* **44**: 764-772.
[34] Aksencer T., Aydogdu M., 2012, Forced transverse vibration of nanoplates using nonlocal elasticity, *Physica E* **44**: 1752-1759.
[35] Daneshmand F., Rafiei M., Mohebpour S.R., Heshmati M., 2013, Stress and strain-inertia gradient elasticity in free vibration analysis of single walled carbon nanotubes with first order shear deformation shell theory, *Applied Mathematical Modelling* **37**: 7983-8003.
[36] Bouyge F., Jasiuk I., Boccara S., Ostoja-Starzewski M., 2002, A micromechanically based couple-stress model of an elastic orthotropic two-phase composite, *European Journal of Mechanics A/Solids* **21**: 465-481.
[37] Bandow S., Asaka S., Saito Y., Rao A., Grigorian L., Richter E., Eklund P., 1998, Effect of the growth temperature on the diameter distribution and chirality of single-wall carbon nanotubes, *Physical Review Letters* **80**(17): 3779-3782.